Journal of Alloys and Compounds 661 (2016) 535–540

Contents lists available at ScienceDirect

Journal of Alloys and Compounds

journal homepage: http://www.elsevier.com/locate/jalcom

Effect of H_3BO_3 addition on the sintering behavior and microwave dielectric properties of wolframite-type $MgZrNb_2O_8$ ceramics

H.T. Wu*, J.D. Guo, J.X. Bi, Q.J. Mei

Shandong Provincial Key Laboratory of Preparation and Measurement of Building Materials, University of Jinan, Jinan 250022, China

ARTICLE INFO

Article history:
Received 15 October 2015
Received in revised form
27 November 2015
Accepted 28 November 2015
Available online 1 December 2015

Keywords:
$MgZrNb_2O_8$
Solid-state method
Microwave dielectric properties
H_3BO_3 addition

ABSTRACT

The effect of H_3BO_3 addition on sintering behavior, microstructure and microwave dielectric properties of $MgZrNb_2O_8$ ceramics was investigated by solid-state method. With H_3BO_3 addition, the densification of $MgZrNb_2O_8$ ceramics was improved significantly, and the τ_f was adjusted to shift toward zero direction. Due to the effect of liquid phase produced from H_3BO_3 addition, the sintering temperature was lowered effectively. The variations in the dielectric constant (ε_r) and the $Q{\cdot}f$ values of the $MgZrNb_2O_8$ ceramics are depended on the amount of H_3BO_3 doping and the sintering temperature. As a result, an optimal microwave dielectric property of $Q{\cdot}f = 58{,}930$ GHz, $\varepsilon_r = 23.72$, and $\tau_f = -13.19$ ppm/°C was obtained for the $MgZrNb_2O_8$ ceramic with 1 wt% H_3BO_3 addition sintered at 1200 °C for 4 h. The relatively low sintering temperature and high dielectric properties in microwave range would make $MgZrNb_2O_8$ ceramics promising for application in electronics.

1. Introduction

Recent days, due to rapid advancement in microwave communication technology, the microwave dielectric ceramics have been studied extensively. Microwave ceramics were used in a wide variety of applications such as resonators, filters, oscillators and antennas in microwave communication devices, and they have also been the basis for the realization of microwave control function [1–4]. In order to meet the demand of miniaturization and integration, it is increasingly needed to expand the search for new microwave dielectric materials, which should have appropriate dielectric constant (ε_r), high quality factor ($Q{\cdot}f$), near-zero temperature coefficient of resonant frequency (τ_f) [5]. Among several kinds of microwave dielectric ceramics with low dielectric constant, wolframite-type $MgZrNb_2O_8$ (MZN) ceramics possess excellent properties, high quality factor combined with appropriate dielectric constant. In our previous study, MZN ceramic prepared by solid-state method was studied to have excellent properties: $\varepsilon_r = 27.08$, $Q{\cdot}f = 29{,}070$ GHz and $\tau_f = -24.31$ ppm/°C [6]. Similarly, Y. Cheng et al. [7] reported that the dielectric properties of $\varepsilon_r = 26$, $Q{\cdot}f = 120{,}816$ GHz and $\tau_f = -50.2$ ppm/°C for the $MgZrNb_2O_8$ ceramics sintered at 1340 °C for 4 h by the solid-state method. S.D. Ramarao and V.R.K. Murthy [8] also reported that the MZN ceramics could be sintered at 1500 °C via the traditional solid-state method and exhibited the microwave dielectric properties: $\varepsilon_r = 9.60$, $Q{\cdot}f = 58{,}500$ GHz and $\tau_f = -31.5$ ppm/°C. However, its sintering temperature was so high, which will limit its practical applications inevitably. Therefore, an increasing number of effective measures are used to solve this problem. Nowadays, there are three different methods used to reduce the sintering temperature of microwave dielectric ceramics: the addition of low-melting glasses [9], preparation in chemical methods [10] and reduction of the size of initial particles [11]. Among the above techniques low-melting glassy additive is a kind of cost-effective technique.

Chemical synthesis was often time-consuming and expensive. In contrast, the addition of low-melting glasses was known to be the most popular method for achieving densified ceramics. Therefore, much attention has been paid to using various sintering aids such as LiF, Li_2CO_3, CuO, B_2O_3, V_2O_5 and Li_2O doping into the dielectric ceramics [12–17] and of all sintering fluxes H_3BO_3 was commonly recognized as a good additive, which was able to reduce the sintering temperature of the ceramics significantly reported by other papers elsewhere [13,18]. However, few researches regarding the H_3BO_3 addition on microwave dielectric properties and microstructure of MZN ceramics has been reported in the literature to date. Therefore, in this paper the H_3BO_3-doped MZN ceramics were synthesized by the solid-state method and the sintering characteristics, microstructure and microwave dielectric properties were also investigated in detail.

---

* Corresponding author.
E-mail address: mse_wuht@ujn.edu.cn (H.T. Wu).

http://dx.doi.org/10.1016/j.jallcom.2015.11.223

2. Experimental procedure

High-purity oxide MgO (99%), ZrO_2 (99.99%), Nb_2O_5 (99.9%) and H_3BO_3 were used as raw materials to synthesize the MZN powders by the solid state method. The raw materials were weighed and mixed according to the formula of $MgZrNb_2O_8$ and the amounts of H_3BO_3-doped were 1wt%, 2.5 wt%, 5 wt%, 7.5 wt% and 10 wt% respectively. The mixed powders were ball-milled for 8 h with distilled water in a nylon container with ZrO_2 balls. All the slurries were dried and pre-sintered at 1050 °C for 4 h to obtain single phase MZN. Then the powders were re-milled for 6 h. The dried powders were mixed with high purity paraffin as a binder at 60 °C, granulated and pressed into cylindrical disks of 10 mm in diameter and about 5 mm in thickness at a pressure of about 200 MPa. These pellets were preheated at 500 °C for 4 h to expel the binder and then sintered at 1050°C–1250 °C for 4 h in air at a heating rate of 5 °C/min.

Phase analysis of samples was conducted with the help of a Rigaku diffractometer (Model D/MAX-B, Rigaku Co., Japan) using Ni filtered CuKα radiation ($\lambda = 0.1542$ nm) at 40 kV and 40 mA settings. Based on XRD analysis, the morphology and particle sizes were examined using a transmission electron microscopy (Model JEOL JEM-2010, FEI Co., Japan) coupled with energy dispersive X-ray spectroscopy (EDS). An network analyzer (N5234A, Agilent Co., America) was used for the measurement of microwave dielectric properties. Dielectric constants were measured using Hakki-Coleman post-resonator method by exciting the TE011 resonant mode of dielectric resonator by using an electric probe as suggested by Hakki and Coleman [19]. Unloaded quality factors were measured using TE01d mode by the cavity method [20]. All measurements were made at room temperature and in the frequency of 8–12 GHz. Temperature coefficients of resonant frequency were measured in the temperature range of 25–85 °C. The apparent densities of the sintered pellets were measured use the Archimedes method (Mettler ToledoXS64).

3. Results and discussion

Due to H_3BO_3 doping, the theoretical density of $MgZrNb_2O_8$ ceramics cannot be calculated accurately. Consequently, radial shrinkage ratio and apparent density were used to characterize the sintering properties in this paper. Fig. 1 shows the shrinking ratio and apparent density of $MgZrNb_2O_8$ ceramics with different amounts of H_3BO_3 addition as a function of sintering temperatures, and the optimal sintering temperature can be obtained through this figure. As shown in Fig. 1(a), the apparent density of MZN ceramics doped with different amounts of H_3BO_3 were all increased gradually with the increase of sintering temperature firstly, and then saturated at 1200 °C, especially for the samples doped with 1 wt% H_3BO_3. The increase in density of MZN ceramics was due to the decrease of pores and the improvement of grains as sintering temperature increasing shown in Fig. 3(a)–(d). When the sintering temperature was over 1200 °C, the apparent density of MZN ceramic doped with 5 wt% H_3BO_3 decreased slightly, which can be attributed to the abnormal grain growth observed in the samples. Compared to the previous study [6], it was demonstrated that the addition of H_3BO_3 was indeed able to reduce the sintering temperature of MZN ceramics significantly for the following explanation. H_3BO_3 will be decomposed to B_2O_3 at 184 °C, and the melting point of B_2O_3 is 445 °C, which forms a liquid phase during the sintering process. During liquid phase sintering, the liquid spreads to cover the solid surfaces, works as the liquid bridge between particles. This decreases the friction among the MZN particles and exerts a capillary force, which can be used to rearrange the particles more easily and enhance the densification process to get maximum packing [21].

With the amounts of H_3BO_3 increasing from 1 wt% to 10 wt%, the apparent density of MZN ceramics sintered at different temperatures were all decreased, which was due to the fact that the grains grew rapidly caused by the excessive liquid phase, the pores cannot be expelled promptly and exist in the bulks as the enclosed pores, and then the apparent density decreased. Thus, it was considered that the small amount of H_3BO_3 doping played an important role in reducing the sintering temperature accompanied with the improvement in the apparent density. For further accurate evaluation of sintering ability, the curves of the diametric shrinkage ratio of the samples were also demonstrated in Fig. 1(b), which showed the similar tendency with these of apparent density. It was indicated that a nearly full densification could be obtained for the samples with 1 wt% H_3BO_3 addition. Based on the above results the optimized sintering temperature was determined to be 1200 °C for the MZN compounds with 1 wt% H_3BO_3 addition. The X-ray diffraction patterns of the $MgZrNb_2O_8$ samples with different amounts of H_3BO_3 additive sintered at 1200 °C is illustrated in Fig. 2. It was found that all the samples showed $MgZrNb_2O_8$ with the space group of P2/c as a main crystalline phase, which was in agreement with the ICSD card of No. 48-0329. And the X-ray

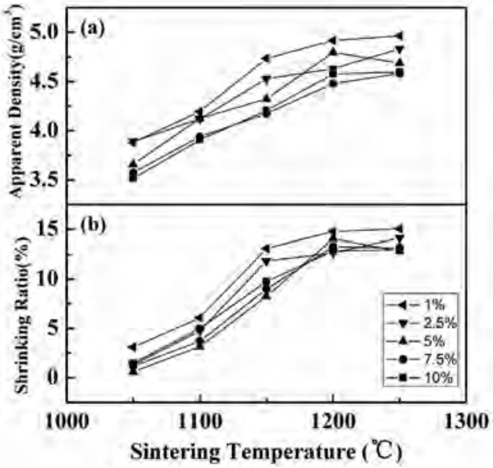

Fig. 1. Shrinking ratio and apparent density of $MgZrNb_2O_8$ ceramics with different amounts of H_3BO_3 addition as a function of sintering temperatures.

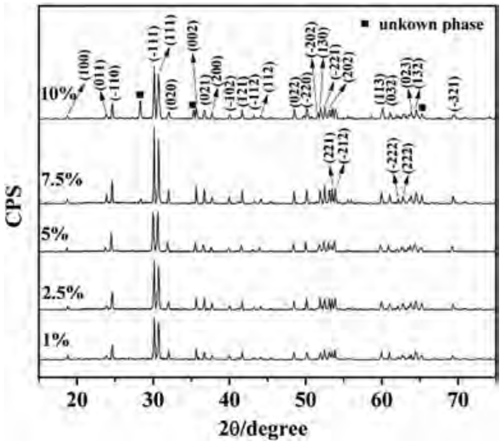

Fig. 2. X-ray diffraction patterns of the $MgZrNb_2O_8$ samples with different amounts of H_3BO_3 additive sintered at 1200 °C.

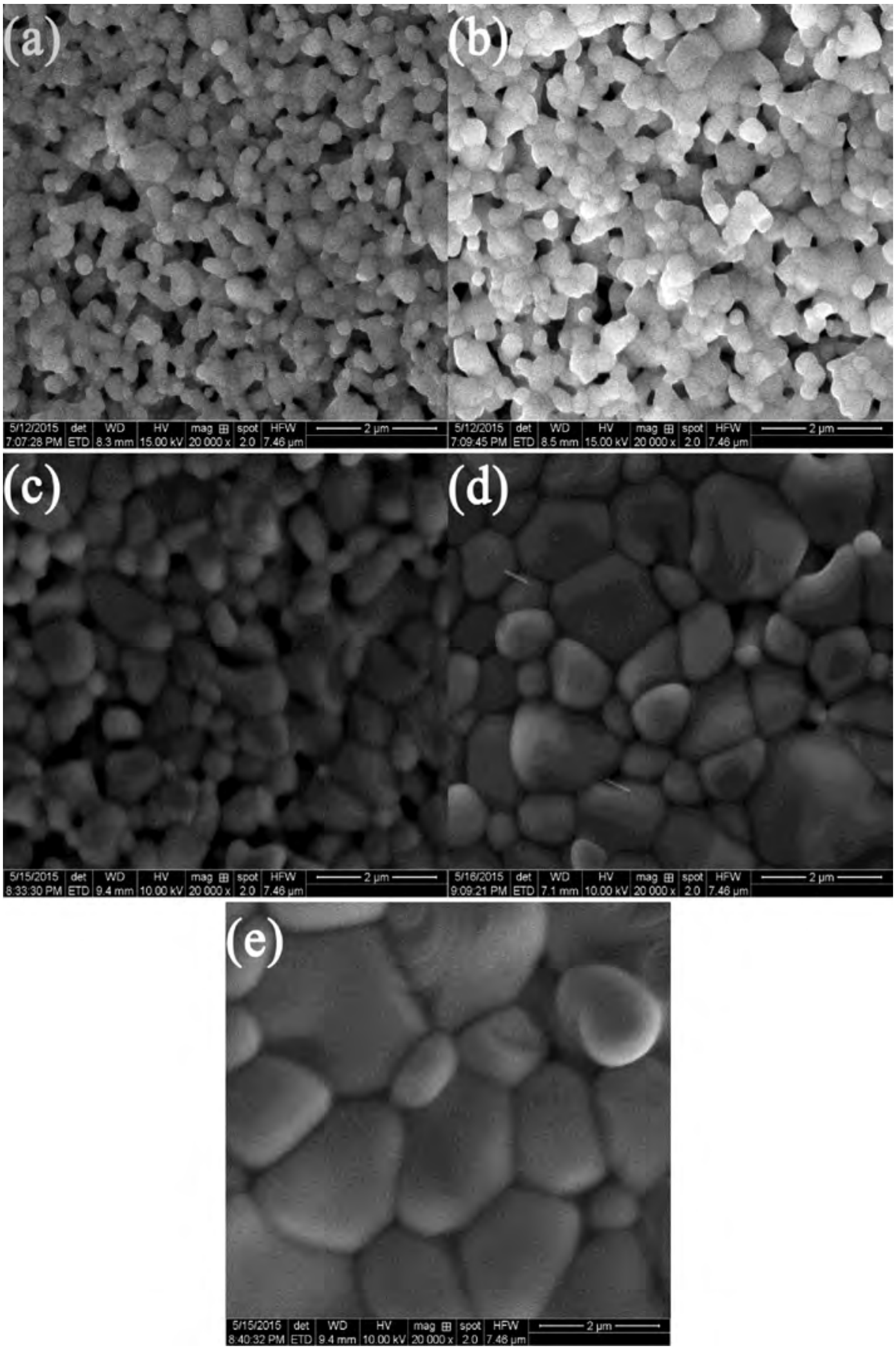

Fig. 3. SEM micrographs of $MgZrNb_2O_8$ samples with 1 wt% H_3BO_3 at different sintering temperatures for 4 h (a–e corresponding to 1050 °C, 1100 °C, 1150 °C, 1200 °C and 1250 °C).

diffraction patterns of MZN ceramics were not changed significantly in different amounts of H_3BO_3 addition. But for the samples doped with 7.5 wt% and 10 wt%, little unknown phase was observed and the diffraction peak intensities of (−111) and (111) were increased significantly. It was discussed that the possible unknown phase existed in the samples doped with 7.5 wt% and 10 wt% may be Boron in that the Boron produced by the excess of H_3BO_3 was not mixed with the main phase of $MgZrNb_2O_8$. And the increasing of peak intensities of (111) and (−111) may be due to the sudden growth of grain shown in Fig. 4(d) and (e).

In order to clarify the effects of sintering temperatures and the amounts of H_3BO_3 doping on the microstructures of $MgZrNb_2O_8$ compounds, the morphological changes in the 1 wt% H_3BO_3-doped $MgZrNb_2O_8$ compounds sintered at different temperatures and samples with various H_3BO_3 addition sintered at 1200 °C are investigated as representatives. The surface micrographs of $MgZrNb_2O_8$ samples with 1 wt% H_3BO_3 at different sintering temperatures are shown in Fig. 3. The 1 wt% H_3BO_3 doping sample sintered at 1050 °C showed spheric-shape grains of quite uniform size (less than 1 μm), with a highly porous microstructure shown in Fig. 3(a). As sintering temperature increased to 1150 °C, the grains grew rapidly and the porosity decreased significantly. All pores almost disappeared at 1200 °C on the surface of 1 wt% H_3BO_3 doping sample. However, when the sintering temperature was over

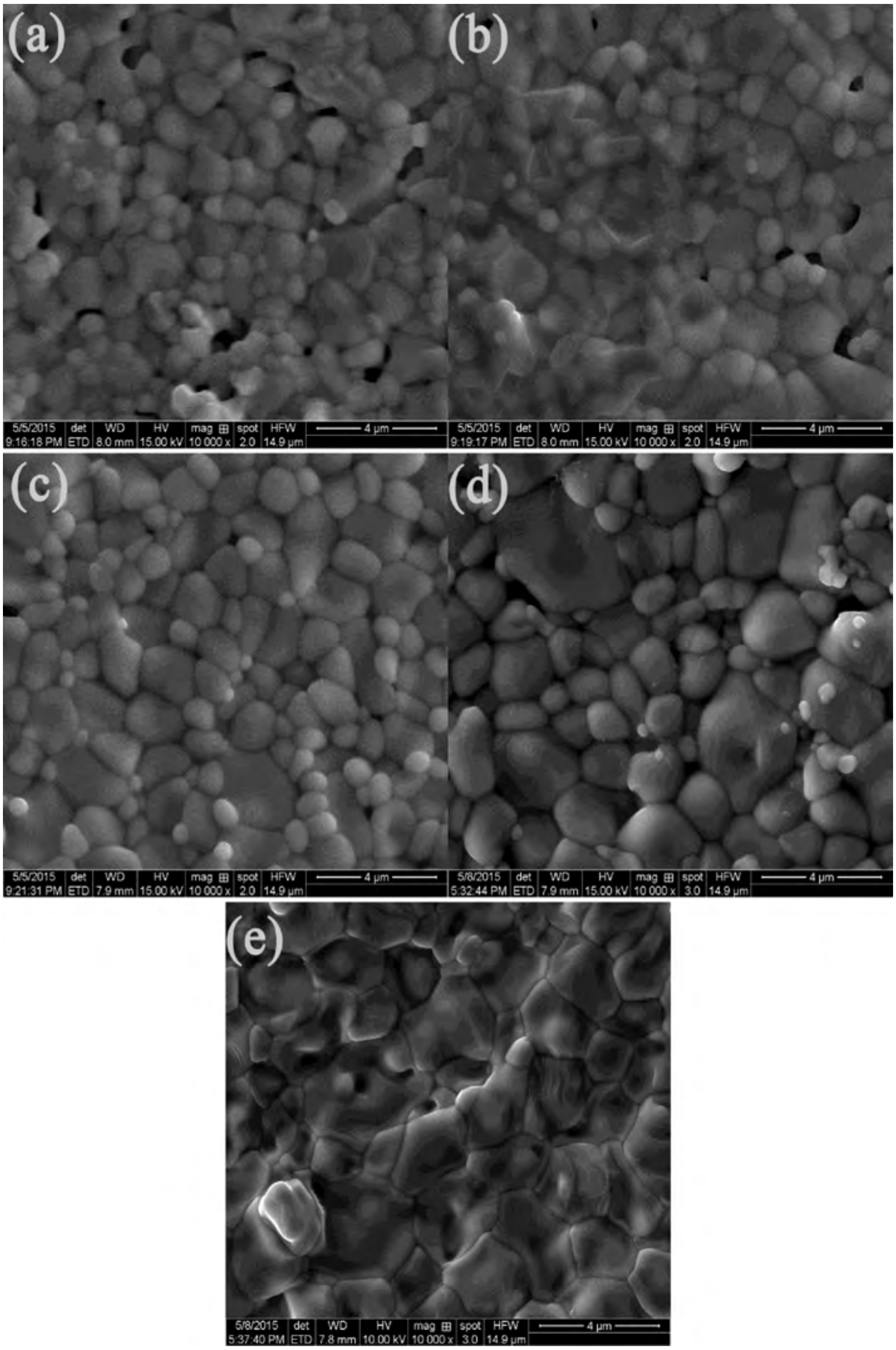

Fig. 4. SEM micrographs of the samples with different amounts of H_3BO_3 doping sintered at 1200 °C (a–e corresponding to 1 wt%, 2.5 wt%, 5 wt%, 7.5 wt% and 10 wt%).

1200 °C, abnormal rapid grain growth appeared shown in Fig. 3(e). Thus, the dense microstructure with low porosity and well-formed spheric-shape grains (1–2 μm) was obtained at 1200 °C shown in Fig. 3(d), which was consistent with the results of the sintering characterization shown in Fig. 1.

Consequently, the surface micrographs of the samples with different amounts of H_3BO_3 doping sintered at 1200 °C are shown in Fig. 4. For the sample with 1 wt% H_3BO_3 addition shown in Fig. 4(a), some grains were structured and the grain boundaries were obvious, but a few of pores were also appeared beside them. However, the grain boundaries of other grains were not obvious as shown in Fig. 4(a). This phenomenon may be due to the segregation resulted from the small amount of H_3BO_3. As the H_3BO_3 content increased, the specimen became well-densified as well as rapid grain growth. Further addition of H_3BO_3 will result in an inferior microstructure as shown in Fig. 4(e). For the MZN ceramic with 10 wt% H_3BO_3 addition, the grains were connected with each other and the grains were melted. Meanwhile, some pores appeared inside the grains, which was due to the fact that the grains grow rapidly caused by the excessive liquid phase, the pores cannot be expelled promptly and exist in the bulks as the enclosed pores. The decrease of apparent density for the MZN ceramic with 10 wt% H_3BO_3 addition shown in Fig. 1(a) was also caused by this reason.

In addition, EDS analysis about grains chosen randomly from the

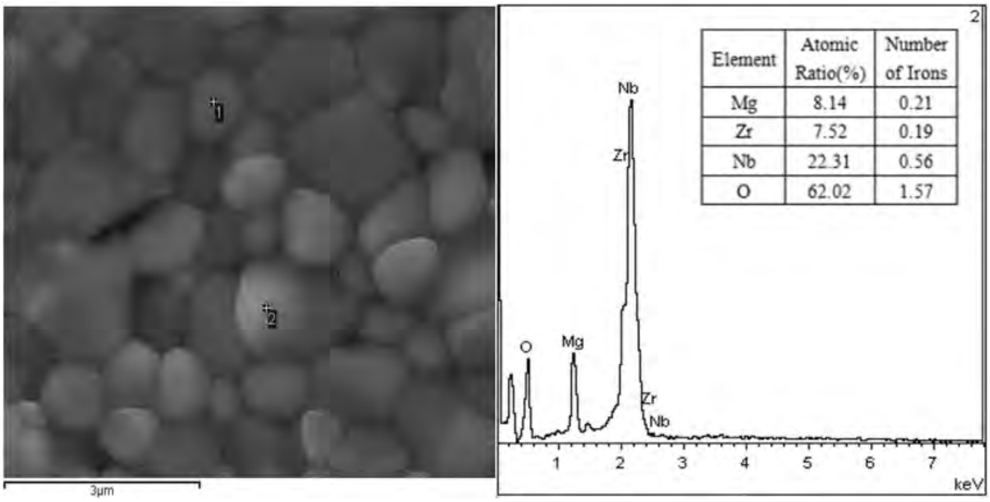

Element	Atomic Ratio(%)	Number of Irons
Mg	8.14	0.21
Zr	7.52	0.19
Nb	22.31	0.56
O	62.02	1.57

Fig. 5. EDS spectrum of $MgZrNb_2O_8$-1 wt% H_3BO_3 ceramic sintered at 1200 °C.

samples with 1 wt% H_3BO_3 sintered at 1200 °C is shown in Fig. 5. The inset in Fig. 5 presents a quantitative result about elementary composition. The atomic ratio of Mg, Zr, Nb and O ions in the grain were analyzed to be 8.14, 7.52, 22.31 and 62.02 at%, respectively. It could be seen that the ratio of Mg:Zr:Nb:O was about 1:0.9:2.74:7.62, which was approximately consistent with the theory composition of $MgZrNb_2O_8$.

Fig. 6 demonstrates the variations of the ε_r and Q·*f* value of the H_3BO_3-added MZN ceramics as a function of sintering temperature and the amount of H_3BO_3. Fig. 6(a) shows that the ε_r values of samples with various amount of H_3BO_3 increased with the sintering temperature increasing from 1050 °C to 1200 °C firstly, and then decreased when the sintering temperature was up to 1250 °C. The increase at first was due to the densification of MZN ceramics, and the decrease in dielectric constant may be ascribed to the abnormal grain growth appearing at higher sintering temperature. For samples sintered at different temperatures, with the increase of H_3BO_3 additions the dielectric constant decreased due to the effect of the lower dielectric constant of H_3BO_3 according to the well-known general empirical model for multiphase ceramics [22]. However, for the MZN ceramics with 10 wt% H_3BO_3 addition sintered at 1050 °C, 1100 °C, 1150 °C and 1250 °C, the dielectric constant increased slightly, which may be due to the unknown secondary phase resulted from the excessive H_3BO_3 addition shown in Fig. 2. For the $MgZrNb_2O_8$-5 wt% H_3BO_3 ceramics sintered at 1050 °C and 1200 °C, the ε_r values also increased slightly caused by the lower porosity and more dense microstructure shown in Fig. 5. Based on the above results, it can be found that the maximum dielectric constant of 23.72 was observed for the sample with 1 wt% H_3BO_3 addition sintered at 1200 °C. In our previous study [6], the dielectric constant value of pure $MgZrNb_2O_8$ ceramic was detected to be 27.08. By comparison, it was seen that the ε_r value of MZN ceramic with 1 wt% H_3BO_3 addition was slightly lower than that of pure MZN ceramic, which may be ascribed to the low ε_r value of H_3BO_3 addition as well as the inferior microstructure caused by the glassy phase of H_3BO_3 addition.

The plots of Q·*f* values of MZN ceramics with different amounts of H_3BO_3 addition as functions of sintering temperature are illustrated in Fig. 6(b). From Fig. 6(b) it can be found that for the samples doped with 1 wt% and 2.5 wt% H_3BO_3 the Q·*f* values increased with the sintering temperature increasing from 1050 °C to 1200 °C. In the same temperature region, the Q·*f* values of MZN ceramics with 2.5 wt%, 7.5 wt% and 10 wt% H_3BO_3 addition decreased slightly first

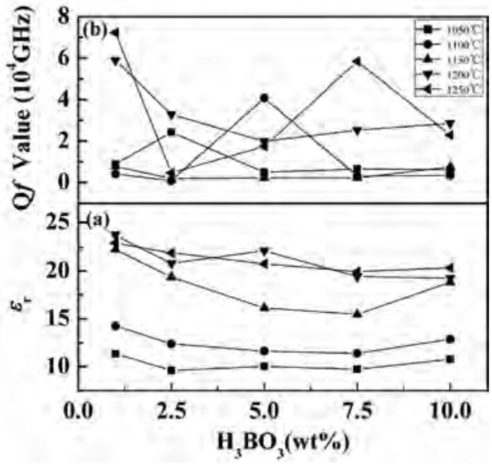

Fig. 6. Variations of the ε_r and Q·*f* value of the H_3BO_3-added MZN ceramics as a function of sintering temperature and the amount of H_3BO_3.

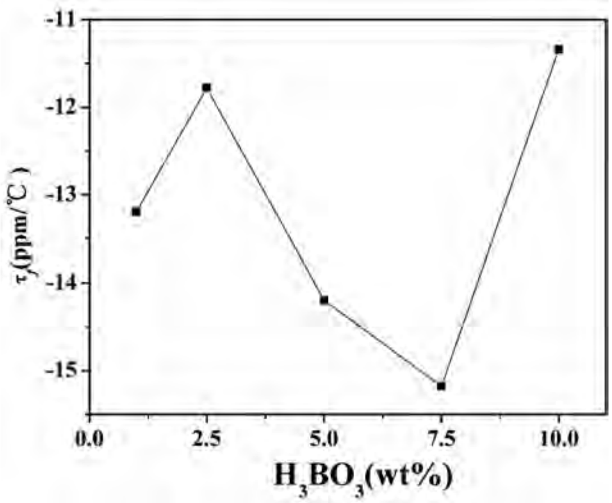

Fig. 7. Temperature coefficient of resonant frequency of MZN ceramics with various contents of H_3BO_3 sintered at 1200 °C for 4 h.

and then increased. When the sintering temperature was over 1200 °C, the Q·*f* values of samples with 1 wt% and 7.5 wt% H_3BO_3 addition were still increased. However, the Q·*f* values of samples with 2.5 wt%, 5 wt% and 10 wt% H_3BO_3 addition were in downtrend. So the maximum Q·*f* value of 58,930 GHz was obtained for $MgZrNb_2O_8$-1 wt% H_3BO_3 doped ceramic sintered at 1200 °C, which was higher than that of pure MZN ceramic of 29,070 GHz [6]. As is known to us, the microwave dielectric loss includes not only intrinsic losses mainly caused by the lattice vibration modes but also extrinsic losses dominated by densification/porosity, the secondary phases, grain sizes and oxygen vacancies [23]. Among these factors, porosity was suggested to affect Q·*f* values obviously below 1200 °C. The remarkable increase in Q·*f* values in the range of 1050°C–1200 °C was associated with the decrease of porosity according to the results of the sintering characteristic curves and SEM microstructure shown in Figs. 1 and 3(a–d), respectively. Some investigations [24,25] also reported that when the relative density was higher than 90%, the Q·*f* value was no longer dependent on density and porosity. That is to say, once the prepared samples reached nearly full density, Q·*f* values were mainly affected by intrinsic factors. So the decrease in Q·*f* values above 1200 °C could be attributed to the non-uniform microstructure caused by abnormal grain growth shown in Fig. 3(e).

As shown in Fig. 6(b), we found that for the samples added with 2.5 wt% H_3BO_3, the maximum Q·*f* value can be obtained for the MZN ceramic sintered at 1050 °C. When the H_3BO_3 addition increased to 5 wt%, the sintering temperature of the sample with the maximum Q·*f* value was increased to 1100 °C. For the samples added with 7.5 wt% H_3BO_3, the maximum Q·*f* value was obtained at 1250 °C. With the increase of H_3BO_3 addition, the temperature of the maximum Q·*f* value shifted toward higher sintering temperatures. For the MZN ceramics sintered at 1150 °C and 1200 °C, the Q·*f* values of MZN ceramics decreased with the amount of H_3BO_3 increasing, which was due to large glassy phase caused by H_3BO_3 doping. As we all know, the large dielectric loss of glassy phase will increase the dielectric loss of the MZN ceramics resulting in the decrease of the Q·*f* values. However, the Q·*f* values increased slightly with the amount of H_3BO_3 increasing from 5 wt% to 10 wt%, which may be attributed to the unknown phase shown in Fig. 2 caused by the reaction of the excessive H_3BO_3 and the predominant phase of $MgZrNb_2O_8$.

Based on the above results, we can find that the optimal sintering temperature was 1200 °C. Therefore, the temperature coefficient of resonant frequency (τ_f) of MZN ceramics sintered at 1200 °C as a function of H_3BO_3 contents were illustrated in Fig. 7. Generally, τ_f is related to the composition, the additives and the secondary phase. It is almost independent on sintering temperature and B_2O_3 content because of no significant compositional change. And all the τ_f values were fluctuated around −13.5 ppm/°C, ranging from −11.34 ppm/°C to −15.18 ppm/°C. As for the sample of MZN ceramic with 1 wt% H_3BO_3 content, the τ_f value was −13.19 ppm/°C. In our previous study [6], the τ_f value of MZN ceramic obtained at 1225 °C was −24.31 ppm/°C. By comparison, it can be found that the τ_f value of MZN ceramic with 1 wt% H_3BO_3 addition was more close to zero, which indicated the better temperature stability. Hence, it was obvious that the improvement in the τ_f value was required for the dielectric resonator applications at high frequency.

4. Conclusions

The effect of H_3BO_3 doping on the microwave dielectric properties and microstructure of $MgZrNb_2O_8$ compounds at various sintering temperatures was investigated by the solid-state method. The XRD patterns of $MgZrNb_2O_8$ compounds with various H_3BO_3 addition showed the ordered wolframite-type structured $MgZrNb_2O_8$ with the space group of P2/c, corresponding to the ICSD card of No. 48-0329, and no secondary phases were observed. The excess of H_3BO_3 doping shown in SEM micrographs and sintering at higher temperatures seemly had a detrimental effect on the microwave dielectric properties. It was found that 1 wt% H_3BO_3 doping was effective in reducing the sintering temperature and improving the Q·*f* value of $MgZrNb_2O_8$ compounds without a slightly decline on dielectric constant. The excellent microwave properties, the Q·*f* value of 58,930 GHz, the ε_r value of 23.72, and the τ_f value of −13.19 ppm/°C were obtained for $MgZrNb_2O_8$ ceramic with 1 wt% H_3BO_3 addition sintered at 1200 °C for 4 h.

Acknowledgments

This work was supported by the Project Development Plan of Science and Technology of Ji'nan City (No. 201303061), Ji'nan City Youth Science and Technology Star Project (No. 2013035), and National Natural Science Foundation (No. 51472108) and Study Abroad Programs by Shandong Province Government.

References

[1] A. Terrell Vanderah, Science 298 (2002) 1182–1184.
[2] R.J. Cava, J. Mater. Chem. 11 (2001) 54–62.
[3] I.M. Reaney, D. Iddles, J. Am. Ceram. Soc. 89 (2006) 2063–2072.
[4] H.T. Wu, L.P. Zhao, J. Univ. Jinan (Sci. Tech.) 30 (2016) 177–183.
[5] M.T. Sebastian, Dielectric Materials for Wireless Communication, Elsevier Science & Technology, 2008.
[6] J.D. Guo, J.X. Bi, Q.J. Mei, et al., J. Alloys. Compd. 655 (2016) 60–65.
[7] S.D. Ramarao, V.R.K. Murthy, Scr. Mater. 69 (2013) 274–277.
[8] Y. Cheng, R.Z. Zuo, Y. Lv, Ceram. Int. 39 (2013) 8681–8685.
[9] T. Takada, S.F. Wang, S. Yoshikawa, et al., J. Am. Ceram. Soc. 77 (1994) 1909–1916.
[10] E.A.V. Ferri, J.C. Sczancoski, L.S. Cavalcante, et al., Mater. Chem. Phys. 117 (2009) 192–198.
[11] K.T. Santhosh, P. Gogoi, A. Perumal, et al., J. Am. Ceram. Soc. 97 (2014) 1054–1059.
[12] Y.Z. Hao, H. Yang, G.H. Chen, et al., J. Alloys. Compd. 552 (2013) 173–179.
[13] W. Wang, L.Y. Li, S.M. Xiu, et al., J. Alloys. Compd. 639 (2015) 359–364.
[14] M. He, H.W. Zhang, J. Alloys. Compd. 586 (2014) 627–632.
[15] T.W. Zhang, R.Z. Zuo, Ceram. Int. 40 (2014) 15677–15684.
[16] C.H. Shen, C.L. Huang, L.M. Lin, et al., J. Alloys. Compd. 489 (2010) 170–174.
[17] S.P. Wu, J.H. Luo, S.X. Cao, J. Alloys. Compd. 502 (2010) 147–152.
[18] P. Zhang, Y.B. Hua, W.S. Xia, et al., J. Alloys. Compd. 534 (2012) 9–12.
[19] B.W. Hakki, P.D. Coleman, IEEE Trans. 8 (1960) 402–410.
[20] W.E. Courtney, IEEE Trans. 18 (1970) 476–485.
[21] W.S. Kim, T.H. Kim, E.S. Kim, K.H. Yoon, Jpn. J. Appl. Phys. 37 (1998) 5367–5371.
[22] W.D. Kingery, Introduction to Ceramics, second ed., Wiley, New York, 1976.
[23] B.D. Silverman, Phys. Rev. 125 (1962) 1921–1930.
[24] W.S. Kim, T.H. Kim, E.S. Kim, et al., Jpn. J. Appl. Phys. 37 (1998) 5367–5371.
[25] C.L. Huang, M.H. Weng, Mater. Res. Bull. 35 (2000) 1881–1888.